13th International Conference on
Structural Health Monitoring of Intelligent Infrastructure
DOI: 10.3217/978-3-99161-057-1-032

Pi-bracket fatigue sensor for crack detection monitoring near stiffeners in bridge girders

B. Telehanic[1,3], A. Mufti[1,3], D. Thomson[2,3], B. Bakht[1,3] and E. Murison[4]
[1]Department of Civil Engineering, University of Manitoba, Winnipeg, Canada
[2]Department of Electrical and Computer Engineering, University of Manitoba, Winnipeg, Canada
[3]SIMTReC Centre, University of Manitoba, Winnipeg, Canada
[4]Manitoba Transportation and Infrastructure, Winnipeg, Canada
email: telehanb@myumaniotba.ca, aftab.mufti@umanitoba.ca, douglas.thomson@umanitoba.ca, bbakht@hotmail.com, evangeline.murison@gov.mb.ca

ABSTRACT: This study investigates an innovative pi-bracket sensor system integrating distributed fiber optic sensing with Brillouin Optical Time Domain Analysis to detect cracks in bridge girders near stiffeners. The system is designed to overcome challenges in crack detection at these critical locations. Experimental validation was conducted on a 3-meter steel beam featuring a welded stiffener positioned 25mm from a simulated crack. An aluminum pi-bracket served as a mounting device for the fiber optic sensor. Comparative analysis between experimental measurements and finite element simulations demonstrated the system's ability to detect crack openings as small as 0.2mm. Abaqus Finite Element Analysis predicted strain values of 145με, while laboratory experiments recorded 129με, a discrepancy of approximately 11%. Strain concentrations were localized to the regions where the pi-bracket was in direct contact with the beam. The strong correlation between computational models and empirical data substantiates the efficacy of the proposed sensing system. These findings highlight the system's potential for structural health monitoring of bridge infrastructure, particularly for detecting and quantifying cracks near stiffeners.

KEY WORDS: Structural health monitoring; Crack detection; Fiber optic sensing; Brillouin optical time domain analysis.

1 INTRODUCTION

Short and medium span bridges are critical components of national transportation networks, significantly contributing to economic activity. As these structures age, they become increasingly vulnerable to structural deficiencies such as reduced load-bearing capacity, accidental damage, material deterioration, fatigue cracking, and foundation problems. Of particular concern is the formation and propagation of cracks in steel bridge girders, which can severely compromise structural integrity [1, 2, 3].

Steel girders, typically constructed from web plates with welded flanges, are fundamental to bridge design, however, they are prone to cracking. These cracks often arise due to cyclic stresses caused by vehicular traffic and environmental factors. Early detection is critical to prevent unexpected service disruptions and mitigate associated economic losses [4, 5].

Advancements in distributed fiber optic sensing (FOS) systems have significantly enhanced the monitoring of bridge structures. However, a critical limitation of this technology is its inability to reliably detect cracks that form near stiffeners, components that are especially susceptible to crack initiation and propagation due to residual stresses, geometric discontinuities from welding, and stress concentrations arising from restricted deformation under repeated loading cycles [8]. Because the FOS is distributed, it is often left unattached in the vicinity of stiffeners, resulting in unmonitored zones extending 5-10 inches on either side of the stiffener, as illustrated in Figure 1. Furthermore, these unattached portions of the FOS lack the support and protection provided by the surrounding structure, rendering them more vulnerable to mechanical damage. These limitations raise concerns regarding the reliability of current monitoring systems in ensuring the structural integrity of steel bridges [1].

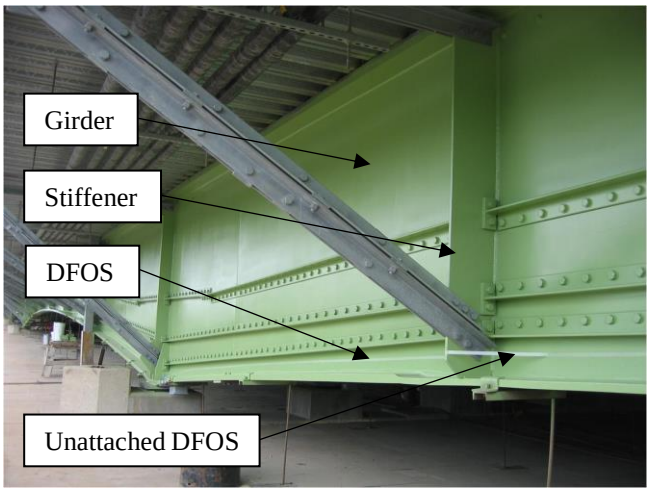

Figure 1. Steel girder with welded stiffener and DFOS in current monitoring system

This study seeks to address these challenges by evaluating a pi-bracket fatigue sensor integrated with FOS technology and Brillouin Optical Time Domain Analysis (BOTDA) for crack detection in steel girders. The pi-bracket serves as protective housing for the FOS, preventing mechanical damage while enabling crack detection near stiffeners. Conventional Structural Health Monitoring (SHM) practices often avoid attaching FOS near stiffeners due to fiber bending constraints, limited space, or risks of mechanical damage during installation.

This research aims to evaluate the pi-bracket sensor system's ability to accurately detect and monitor cracks in critical areas of a simulated bridge girder and compare its performance with

DOI: 10.3217/978-3-99161-057-1-032

Finite Element Analysis (FEA) predictions. Ultimately, this study aims to advance the development of more reliable SHM systems, promoting enhanced safety, proactive maintenance, and extended service life for bridge structures.

2 METHODOLOGY AND EXPERIMENTAL SETUP

2.1 FEA Model

A three-dimensional finite element model was developed using ABAQUS to simulate the experimental setup (Figure 2). The model consisted of three main components: the steel girder, aluminum pi-bracket, and steel stiffener, all modeled as deformable planar shell elements with thicknesses corresponding to experimental dimensions (8.9mm for girder web, 15.7mm for girder flanges, and 3.175mm for pi-bracket). Two distinct material properties were incorporated: steel and aluminum. The simulation focused on the linear elastic behavior within the elastic region of the elastic-plastic relationship, defining only Young's modulus and Poisson's ratio for both materials. Aluminum was characterized by a Young's modulus of 69000 MPa and a Poisson's ratio of 0.33, while steel was defined by a Young's modulus of 210000 MPa and a Poisson's ratio of 0.3.

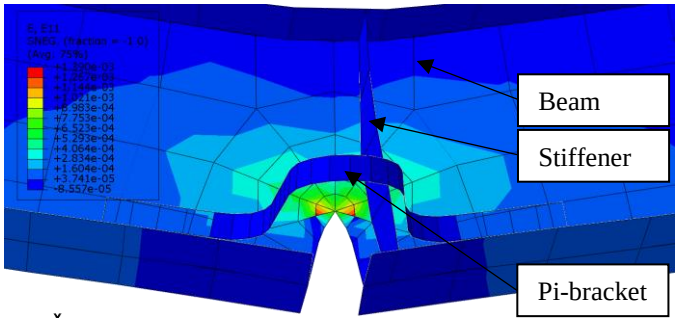

Figure 2. FEA model of the beam with the stiffener crack and pi-bracket.

The connections in the ABAQUS model between the FOS, pi-bracket, and beam were modeled as rigid interfaces using tie constraints. This modeling approach enforces identical displacements and rotations at the interface, effectively simulating a completely rigid bond between the connected components. Although this represents an idealized scenario, it is sufficient for the purposes of this study, which focuses on the ability to detect the initiation of cracks.

Regarding fiber rupture concerns, our detection system targets very small crack openings, significantly below thresholds that would risk fiber damage. Even in the unlikely event of rupture due to extreme crack propagation, the distributed nature of the FOS (with its dense sampling points) would instantly identify the failure location, enabling immediate inspector dispatch for visual assessment. This aligns with the research objective: developing a continuous monitoring system for early crack detection to support timely intervention and maintenance.

To simulate a simply supported 3-meter steel girder, appropriate boundary conditions were applied to each end of the beam. A pinned support at one end restricted U1, U2, U3, UR2, and UR3, while a roller support at the other end allowed axial displacement. The crack was explicitly defined as a stationary geometric discontinuity using a face partition at the beam's midspan web location, extending 57mm vertically from the bottom edge of the web. The crack was defined as a contour integral, with the crack extension direction specified by selecting q-vectors. The singularity was modeled as a collapsed element side with a single node, with the mid side node parameter set to 0.3 to accurately capture the stress singularity.

The simulation employed displacement-controlled loading (crack opening 0.1mm and 0.2mm), with concentrated forces applied at the midspan of the beam. The applied displacement was defined as the relative movement between two nodes located at the same height as the pi-bracket, on either side of the crack. This approach does not imply that the entire crack opens uniformly by the prescribed amount. Instead, the displacement at the crack tip remains zero, while the maximum opening occurs at the bottom of the web, between the flanges. For example, when a 0.2 mm displacement is specified the actual opening at the crack tip is zero, and the opening at the bottom of the web is larger.

The model was primarily meshed using Quad 4-node shell elements (S4R), with Tri 3-node shell elements (S3) used in areas surrounding the crack. The S4R element is a general-purpose quadrilateral element suitable for large-strain analysis, featuring six degrees of freedom per node with bilinear interpolation.

This FEA model configuration enables accurate simulation of the beam's behavior under specified loading conditions, allowing detailed analysis of stress distributions and deformations, particularly in critical regions surrounding the crack and pi-bracket. The objective was to assess the pi-bracket sensor system's ability to detect strain changes resulting from crack formation, aligning with the study's focus on evaluating sensor performance for SHM applications.

2.2 Experimental Setup

The test configuration used a W250x67 (W10x45) structural steel beam in a simply supported arrangement spanning 3 meters to replicate typical in-service conditions (Figure 3). A controlled crack was introduced at midspan through precision machining, extending through the bottom flange and vertically 57 mm into the web from the beam's underside.

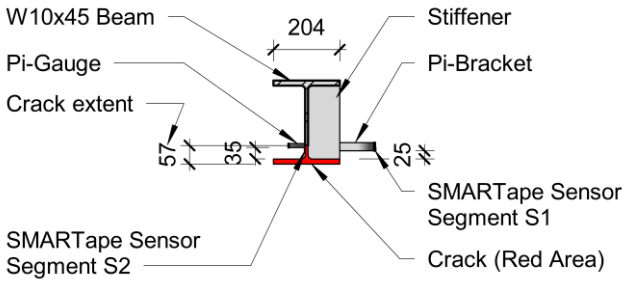

Figure 3. Beam - Section.

To simulate realistic bridge girder geometry, a transverse stiffener was welded to the beam 25 mm from the crack edge on one side. This asymmetric design was chosen to generate asymmetric stress distributions characteristic of operational bridge environments, and to allow a comparative assessment between stiffened and non-stiffened regions.

The pi-bracket assembly was installed at a vertical offset of 35 mm above the bottom flange's upper edge, with its central axis aligned to the stiffener position (Figure 4). This spatial

DOI: 10.3217/978-3-99161-057-1-032

configuration was optimized to facilitate sensor routing while maintaining proximity to critical stress zones, enhancing detection sensitivity to crack-induced strain fields. The geometry of the stiffener, crack location, and pi-bracket placement were designed to emulate common failure scenarios observed in aging bridge infrastructure.

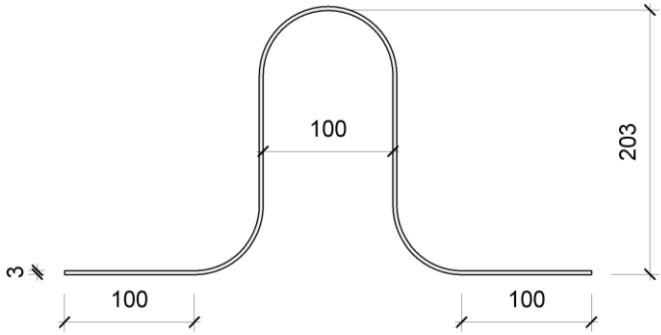

Figure 4. Pi-bracket geometry.

2.3 Instrumentation

The primary sensing technology used in this study was the DiTeSt SMARTape II fiber optic sensor, developed by Smartec. This high accuracy distributed strain sensor, comprising a single continuous optical fiber, was adhered to both sides of the beam using epoxy adhesive. On the front face, the sensor was routed over the simulated crack using the Pi-Bracket, which acted as a protective harness (Figure 5a). In contrast, on the rear face, the sensor was directly bonded to the surface of the beam, passing through the crack region (Figure 5b). Fiber continuity was ensured by routing it back at one end of the beam to transition from the front to the rear face.

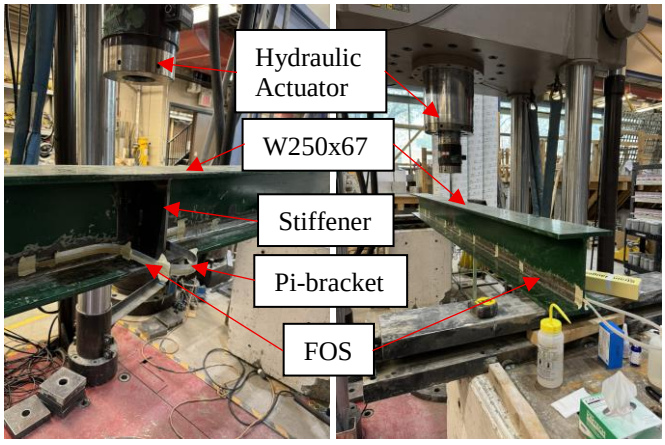

a) b)

Figure 5. a) SMARTape on the front face; b) SMARTape on the rear face.

The termini of the SMARTape sensor were fusion spliced to extension fiber optic cables and connected to a Data Acquisition (DAQ) system, enabling real-time monitoring and data collection throughout the experiment. Various configurations of the Neubrescope NBX-6050 DAQ system were tested to identify optimal parameters prior to this experiment. The optimal configuration utilized a 5 cm sampling interval and a 10 cm spatial resolution. This system used BOTDA technology to achieve high-resolution strain distribution measurements along the length of the FOS.

In the context of steel bridges, critical fatigue cracks are typically considered to be those with widths in the range of 0.1 mm to 0.3 mm, as cracks within this interval are generally regarded as significant for early intervention and maintenance [10]. According to the manufacturer's specifications, the DiTest SMARTape II fiber optic sensor can detect cracks as small as 0.2 mm, and we anticipated that the proposed pi-bracket system would achieve comparable performance. It is important to note that the objective of this study is to evaluate the ability of the pi-bracket sensor system to accurately detect and monitor the presence of cracks, rather than to quantify their exact widths. The primary goal is to determine whether the system can detect the initiation of a crack and enable the immediate intervention of an inspector for further evaluation. This approach supports proactive maintenance and timely intervention, which are critical for ensuring the safety and longevity of bridge infrastructure.

2.4 Fiber Optic Sensor Calibration

The initial strain measurements lacked sufficient resolution to clearly identify the positions of the beam and pi-bracket along the FOS, as shown in Figure 6.

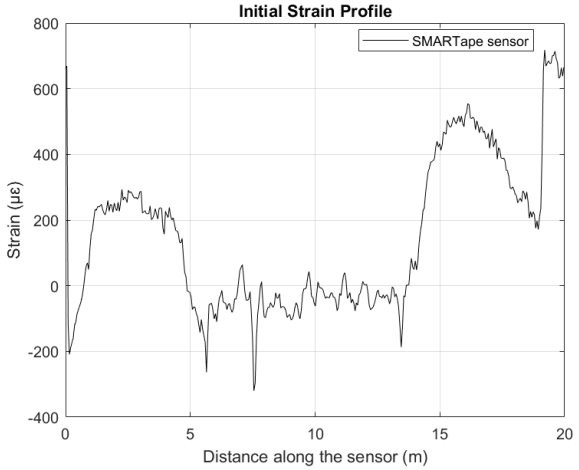

Figure 6. Initial calibration strain profile.

To address this limitation, a thermal localization method was used to enhance spatial resolution and accurately determine key positions. This involved applying localized heat to specific points on the beam, including both ends and the pi-bracket apex. The resulting strain response was recorded and compared to the initial unheated strain profile to isolate the thermal effect.

Thermal localization was employed to precisely determine the positions of the beam faces and the pi-bracket along the FOS strain profile (Figure 7). In the experimental setup, a single, continuous SMARTape sensor was routed from the front to the rear face of the beam, enabling comprehensive strain measurements across the entire structure. By applying thermal localization, the locations of key structural features, such as the front face, back face, and the pi-bracket, were accurately mapped onto the strain profile. Specifically, Sensor S1 corresponded to the portion attached to the front of the beam, spanning from 5.75 meters (A) to 9.35 meters (C) along the sensor length, with the pi-bracket located at 7.55 meters (B). Sensor S2 referred to the segment affixed to the rear of the

DOI: 10.3217/978-3-99161-057-1-032

beam, extending from 10.25 meters (D) to 13.25 meters (E), with the crack opening situated at 11.75 meters.

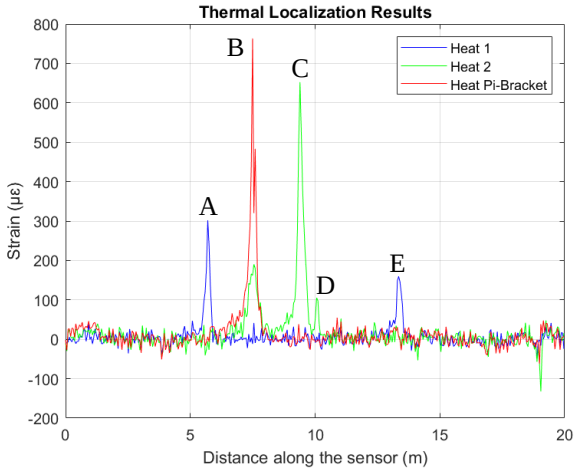

Figure 7. Thermal localization of FOS segments.

Figure 8 provides a comprehensive schematic representation of the entire FOS configuration, illustrating the spatial relationships between the SMARTape II sensor and the pi-bracket.

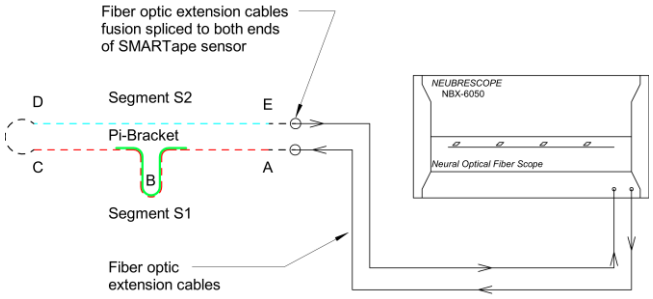

Figure 8. Schematic diagram of fiber optic sensor.

2.5 *Experimental Procedure*

The experimental protocol was designed to rigorously assess the efficacy of the FOS and pi-bracket for crack detection and monitoring. This process involved a sequence of executed stages, beginning with initial configuration and calibration. The experimental apparatus, comprising the beam, pi-bracket with attached FOS and pi-gauge, was interfaced with the DAQ system. The Neubrescope NBX-6050 was adjusted to its optimal parameters, and the FOS was calibrated to ensure measurement accuracy.

According to the manufacturer's specifications, the DiTest SMARTape II fiber optic sensor can detect cracks as small as 0.2 mm [6]. We anticipated that the proposed pi-bracket system would achieve comparable performance. The static load experiment was conducted under controlled laboratory conditions at an ambient temperature of 19.8°C. The crack opening was controlled by a pi-gauge (PI-5-100, Tokyo Sokki Kenkyujo) with a resolution of 0.001 mm and an accuracy within ±1% according to the manufacturer, which was installed at the same height as the pi-bracket to ensure precise crack width [9]. Strain data from the SMARTape sensor were collected for the no-crack condition (referred to as the "initial crack"), as well as for crack opening widths of 0.1 mm and 0.2 mm, with baseline readings taken before load application.

A hydraulic actuator applied midspan loading to induce crack opening. The experiment used displacement control, pausing at a 0.1 mm crack width to record load and beam displacement data (Table 1). Strain measurements were taken at this point. The load was then increased to achieve a 0.2 mm crack width, where additional readings were obtained. Multiple measurements were taken and averaged to generate strain profiles for each crack opening width.

3 RESULTS AND DISCUSSION

3.1 *FEA Results*

The FEA model developed in Abaqus was used to simulate the experimental setup and to investigate the strain behavior of the pi-bracket sensor system under controlled crack opening conditions. This modeling enabled a detailed examination of strain patterns along the FOS.

Two distinct strain profiles were analyzed, as shown in Figure 9. The first strain profile (blue line in Figure 9) represents a scenario without the pi-bracket, reflecting current SHM practices where a continuous FOS is left unattached near stiffeners, resulting in an unmonitored zone of about 10 cm on each side due to installation constraints. This profile serves as a baseline for comparison, illustrating the strain distribution in the absence of the pi-bracket's influence.

The second profile (red line in Figure 9) incorporates the pi-bracket, capturing strain measurements continuously along the entire beam span, including the areas near stiffeners. The green vertical lines in Figure 9 identify the position of the pi-bracket along the strain profile, providing spatial reference points for interpreting the sensor configuration.

To match the DAQ averaging from the experiment, strain profiles were averaged between two points along the path.

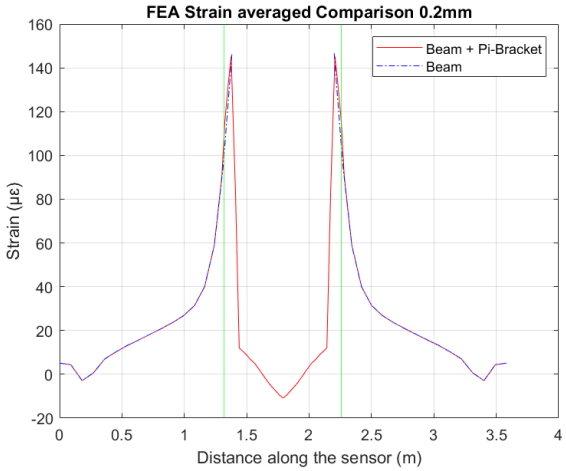

Figure 9. FEA strain profiles for 0.2mm crack: Comparison of Beam with and without Pi-Bracket.

Figure 9 demonstrates that the pi-bracket allows for uninterrupted strain monitoring across the region near the stiffener and crack, effectively eliminating the unmonitored gaps seen in the baseline scenario. Specifically, the region between 1.3 m and 2.2 m along the sensor corresponds to the segment of the FOS routed through the pi-bracket for the second modeled scenario. In contrast, for the first scenario

DOI: 10.3217/978-3-99161-057-1-032

without the pi-bracket, the strain profile is interrupted to reflect current practice where the FOS is left unattached to the surface near stiffeners and therefore does not register any strain in these regions.

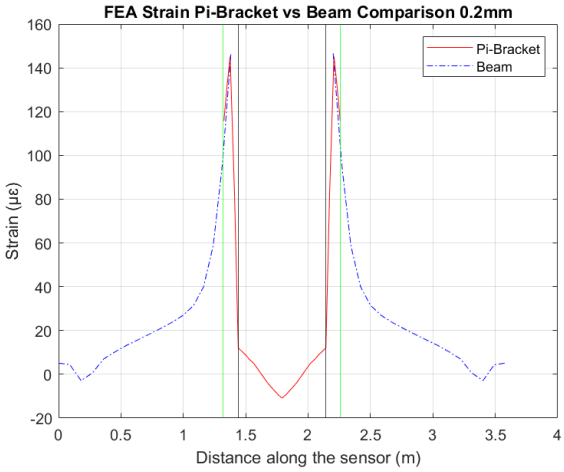

Figure 10. FEA strain profile of Pi-Bracket for 0.2mm crack: Identification of contact and non-contact Pi-Bracket regions.

Figure 10 further isolates the strain response of the pi-bracket section from the overall profile shown in Figure 9, again for a 0.2 mm crack opening. In this figure, black vertical lines indicate the portions of the pi-bracket that are not attached to the beam, while the areas marked by green vertical lines on either side represent the sections of the pi-bracket that are glued to the beam. This distinction is important for interpreting the strain distribution, as the attached and unattached regions of the pi-bracket exhibit different mechanical behaviors due to their interaction with the beam.

For further clarification, Figure 11 provides a schematic of the pi-bracket, highlighting the attached and unattached regions relative to the beam, which aids in interpreting the strain profiles in Figures 9 and 10.

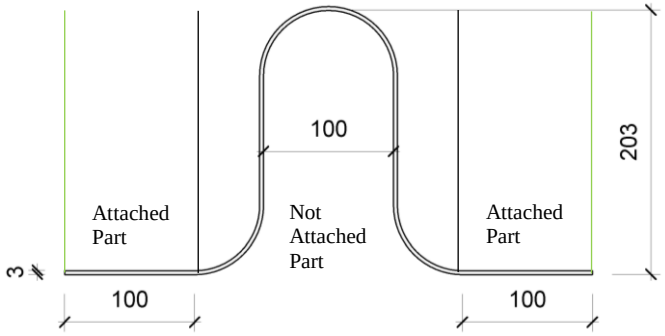

Figure 11. Pi-bracket – part identification

These FEA results demonstrate the effectiveness of the pi-bracket in capturing and distributing strain from the crack region, allowing for continuous monitoring even near critical features such as stiffeners. This provides a valuable reference for comparison with the experimental data.

3.2 Experimental Results

The experimental phase of this investigation yielded extensive strain data collected by the SMARTape FOS system. These measurements provide valuable insights into the performance of the pi-bracket sensor configuration under controlled crack propagation conditions. Figure 12 displays the averaged strain profiles derived from multiple measurements, showing the sensor's response to progressive crack opening widths of 0.1 mm and 0.2 mm, as well as the initial state with no crack for direct comparison before and after crack initiation. The green vertical lines in Figure 12 identify the strain segments S1 and S2: S1 corresponds to the front face of the beam, where the FOS is routed via the pi-bracket, and S2 corresponds to the back face of the beam, where the FOS is attached directly over the crack (since there was no stiffener on this side). This setup, with the stiffener welded to one side only, allows for a direct comparison of the strain profiles between both regions.

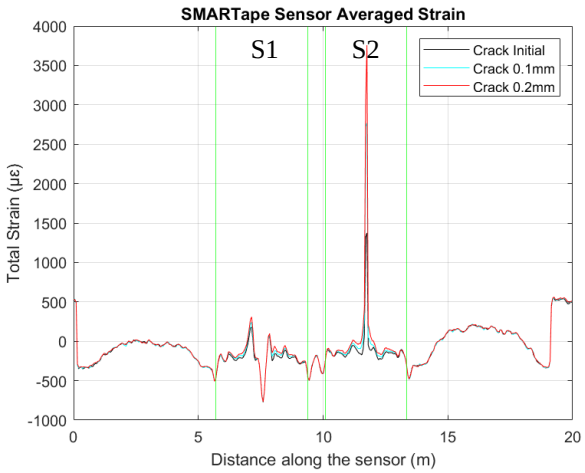

Figure 12. SMARTape averaged strain profiles.

Figure 13 presents the strain profiles obtained by subtracting the initial strain profile (no crack condition) from those measured at 0.1 mm and 0.2 mm crack openings. This approach isolates the strain response resulting specifically from crack widening, eliminating any residual or pre-existing strains within the FOS. The data indicates a significantly higher strain value (2382.1 με) recorded by the sensor section S2, which was directly bonded over the crack, compared to the maximum strain recorded by sensor section S1, distributed over the pi-bracket (129.1 με). All the results are summarized in Table1.

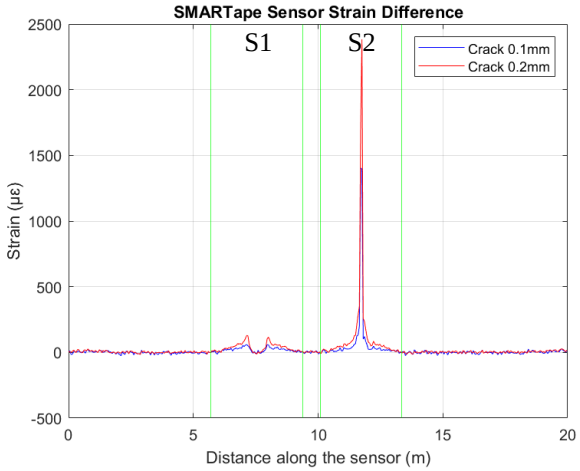

Figure 13. SMARTape strain profiles isolating crack-induced strain.

DOI: 10.3217/978-3-99161-057-1-032

Table 1. Experiment and FEA Results.

Experiment						FEA Simulation		
Crack width [mm]	Load [kN]	Beam displacement [mm]	S1 Strain max. [με]	Strain Pi-Bracket Crown [με]	S2 Strain max. [με]	Strain Pi-Bracket Crown [με]	Strain Pi-Bracket max. [με]	Strain Beam no bracket max. [με]
0	0	0	0	0	0	0	0	0
0.1	15.9	-1.26	60.6	-8.3	1402.9	-5.4	72.95	73.7
0.2	31.9	-2.38	129.1	-11.04	2383.1	-10.8	145.14	146.6

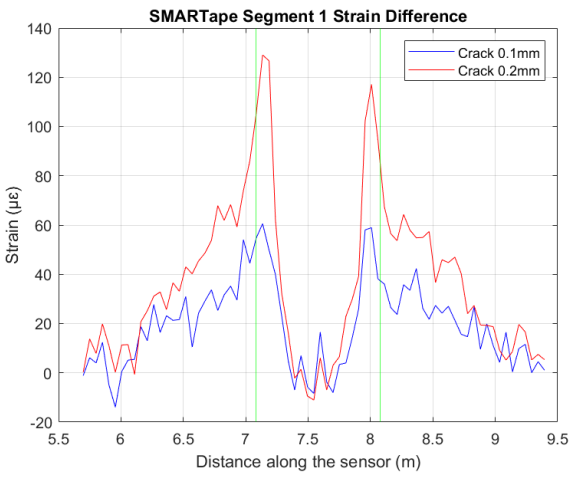

Figure 14. Detailed strain profiles for Section S1.

Figure 14 presents a detailed analysis of the strain profiles for section S1, which includes the pi-bracket at its center. The green vertical lines indicate the position of the pi-bracket along the strain profiles. Although the data exhibits some residual noise, the overall trends in the strain profiles demonstrate the sensor's capacity to detect strain changes induced by crack opening, even when mediated by the pi-bracket. Potential sources of noise include environmental vibrations and temperature fluctuations. The data from S1 provides insights into how the pi-bracket influences strain distribution compared to the direct measurement at the crack location (S2).

3.3 Comparison

This section presents a comparative analysis of experimental results obtained from SMARTape sensor measurements and FEA predictions, evaluating the efficacy of the pi-bracket sensor system for crack detection near stiffeners. The comparison focuses on strain measurements at critical locations, specifically the pi-bracket and crack-adjacent regions (Figures 15, 16).

FEA simulations predicted a maximum strain of 145.1 με in the pi-bracket at the location of direct beam attachment for a 0.2 mm crack opening. Experimentally, the maximum strain recorded by sensor section S1, distributed over the pi-bracket, was 129.1 με for an equivalent crack opening (Figure 15). Again, the green vertical lines indicate the position of the pi-bracket along the strain profile. This represents an approximate 11% discrepancy between the FEA prediction and the experimental measurement. The observed level of agreement suggests that the numerical model adequately predicts the strain behavior of the pi-bracket under the applied loading conditions.

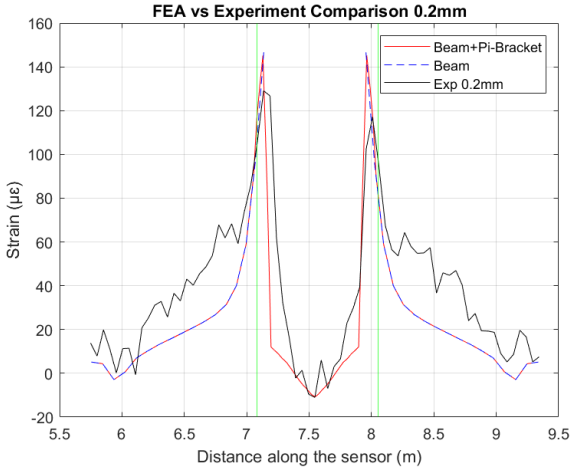

Figure 15. FEA vs Experiment comparison for 0.2mm crack.

Figure 16 presents the same strain results as Figure 15 but focuses exclusively on the strains within the pi-bracket for both the FEA simulations and laboratory experiment at a 0.2 mm crack opening.

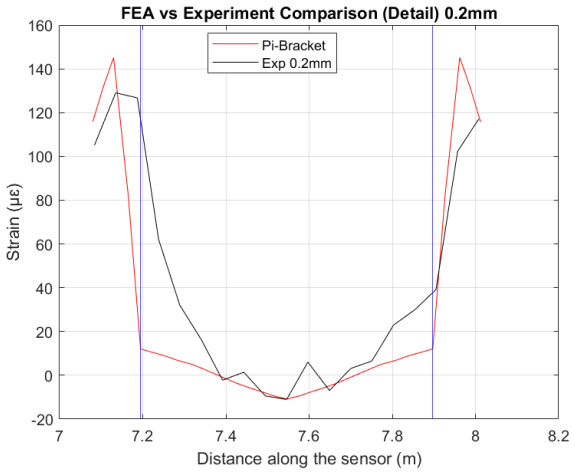

Figure 16. FEA vs Experiment comparison of Pi-Bracket for 0.2mm crack.

DOI: 10.3217/978-3-99161-057-1-032

Figure 16 illustrates the separation of the unattached central region of the pi-bracket from the beam by blue vertical lines, distinguishing it from the attached areas on either side. The FEA predicted a maximum strain of -10.8 με at the crack tip for a 0.2 mm crack opening. Experimentally, the SMARTape sensor section S1 recorded a strain of -11.04 με at the pi-bracket crown (Figure 15), demonstrating close agreement with the FEA results.

Although the strain magnitudes at the pi-bracket crown were relatively small compared to those measured directly over the crack (2383.1 με), the SMARTape sensor affixed to the beam-bonded portions of the pi-bracket successfully detected the crack, registering strains of 129.1 με versus 145.1 με predicted by FEA. This 11% discrepancy validates the numerical model's capability to simulate the pi-bracket's behavior under crack propagation while highlighting the sensor system's sensitivity.

Key Findings:

Validation of Computational Framework: The strong correlation between experimental strain measurements (129 με) and FEA predictions (145 με) confirms the reliability of the numerical model in representing the pi-bracket response to crack-induced strain.

Strain Gradient Localization: Elevated strain values were predominantly localized at the crack interface, with sensor section S2 (directly over the crack) showing significantly higher strains than section S1 (pi-bracket region). This confirms the influence of geometric discontinuities on strain distribution.

Detection Validation: The pi-bracket sensor system demonstrated sufficient sensitivity to detect crack initiation, with strain magnitudes large enough to be readily observed.

Pi-Bracket Efficacy: The pi-bracket functions effectively as both a strain-transfer mechanism and a protective interface for the fiber optic sensor, supporting its potential integration into SHM systems.

The observed 11% difference between experimental and simulated strains can be attributed to simplifications in the FEA model, real-world experimental factors such as sensor performance and data acquisition variability, and mesh density limitations imposed by the software version used. Despite these factors, the overall agreement substantiates the pi-bracket sensor system's effectiveness for crack detection in bridge girders.

Despite these discrepancies, the overall agreement between the experimental results and FEA predictions validates the effectiveness of the pi-bracket sensor system for crack detection in bridge girders. The observed 11% discrepancy suggests that simulation captures experimental behavior with reasonable accuracy, as expected.

3.4 Advantages of the Pi-bracket Sensor System

The pi-bracket sensor system provides improved accuracy in detecting cracks near stiffeners, which are typically challenging to monitor. It functions as a protective harness, shielding the continuous FOS from mechanical damage, a common issue when sensors are left unattached around stiffeners due to bending limitations. This design enables uninterrupted and direct strain measurements along the entire length of the girder, including critical regions near stiffeners.

By integrating BOTDA technology, the system simplifies data acquisition and demonstrates strong alignment with FEA predictions. This combination offers a reliable and efficient approach for validating computational models and facilitating proactive bridge maintenance strategies.

3.5 Real-World Applicability, Limitations, and Capabilities

The findings of this study highlight the potential of the pi-bracket sensor system for practical application in bridge infrastructure, particularly for monitoring high-risk areas near stiffeners. The system is recommended for use in both new bridge construction and retrofitting existing structures to enable targeted monitoring of these critical regions. Its localized measurement capability allows for deployment in areas prone to cracking, while the pi-bracket serves as a protective harness for the FOS.

It should be emphasized, however, that the authors do not recommend the use of this system for monitoring existing cracks. Given the higher cost of FOS compared to conventional methods such as strain gauges, it is not cost-effective for short-term monitoring where the sensor would be installed, the crack repaired at some point, and then the sensor removed or replaced. Instead, this system is best suited for long-term, continuous monitoring, where the FOS is permanently attached to the surface of the girder. This makes it particularly advantageous for bridges that are approaching or have exceeded their intended service life, especially in cases where local authorities lack the financial resources for comprehensive retrofitting or replacement. In such scenarios, the pi-bracket sensor system provides a cost-effective solution for ongoing structural health monitoring, enabling proactive maintenance and extending the operational lifespan of critical infrastructure. Furthermore, the system is well-suited for deployment immediately following crack repair, to monitor the repaired region and prevent recurrence.

It is important to recognize that this system has certain limitations. The installation process can be complex, and environmental factors may influence performance. Additionally, the initial cost of implementation may exceed that of traditional methods, although the long-term benefits could outweigh these expenses. Furthermore, experimental validation was limited to a single beam, necessitating further testing on larger-scale structures to confirm its effectiveness.

Despite these constraints, the pi-bracket sensor system offers several advantages, including accurate crack detection, quantitative strain measurement, remote monitoring capabilities, and integration with FEA models. Its protective design enhances sensor durability and reliability. These attributes make it a valuable tool for improving crack detection in bridges, contributing to enhanced safety, reliability, and longevity of critical infrastructure.

While the initial cost of the pi-bracket FOS system may exceed that of traditional methods, its long-term benefits provide significant value. The system enables continuous, real-time monitoring of strain and crack development, allowing for early detection and timely maintenance interventions that enhance structural safety and reliability. This proactive approach helps extend the service life of

DOI: 10.3217/978-3-99161-057-1-032

bridges by preventing severe damage and delaying costly retrofits or replacements. Additionally, continuous monitoring reduces the need for frequent manual inspections, lowering maintenance costs and minimizing traffic disruptions. The protective design of the pi-bracket also improves sensor longevity, reducing replacement frequency.

It is essential to emphasize that the primary objective of this study was not to investigate fracture mechanics or crack interaction phenomena but rather to evaluate the pi-bracket sensor system's ability to detect early-stage cracks. This capability facilitates preventative measures against potential structural failures in bridge infrastructure.

Given the limitations of existing inspection protocols [3, 7], which rely heavily on periodic manual assessments, this system offers a continuous real-time monitoring solution. It enables immediate crack detection and automated alert generation, allowing for timely deployment of inspectors for detailed visual examination and initiation of necessary repairs.

To address challenges associated with fatigue loading and environmental variations in real-world conditions, future implementations could incorporate frequent data acquisition (e.g., every five minutes). By subtracting consecutive strain measurements, the system could isolate strain changes attributable solely to crack formation while minimizing the influence of dynamic bridge responses or environmental factors. Further investigation is needed to validate this differential approach under complex loading scenarios. Additionally, research should explore the effects of temperature fluctuations and determine optimal averaging times to enhance accuracy and reliability.

3.6 Recommendations for Future Research

Future research should refine the FEA model with higher-resolution meshing to better match experimental results. The pi-bracket system also requires testing under dynamic and fatigue loading, ideally on full-scale bridges, to evaluate durability and real-world performance. Laboratory testing at a constant 19.8°C does not account for temperature variations; therefore, it is recommended to assess temperature effects to distinguish them from crack-induced strains. Additionally, future work should address detection threshold quantification and evaluate false-alarm rates. Developing standardized mounting protocols, including adhesive choice and bracket alignment, will improve field deployment consistency. Finally, cost-benefit analyses comparing system costs to savings from early crack detection are essential to support practical adoption.

4 CONCLUSIONS

This study demonstrates the efficacy of the pi-bracket sensor system as a viable method for crack detection near stiffeners in bridge girders, exhibiting reliable detection capabilities for crack opening widths of 0.2 mm. The FOS distributed over the Pi-bracket recorded a strain of 129 με at a 0.2 mm wide crack opening. Comparative analysis between FEA and laboratory experiments utilizing a FOS provided significant insights into the pi-bracket sensor's performance. The concordance between experimental results and Abaqus simulations corroborates the system's effectiveness and reliability, illustrating the robustness of both the sensor and the modeling approach employed for design optimization.

The pi-bracket configuration successfully addresses the challenge of monitoring traditionally inaccessible areas near stiffeners, while the integration of BOTDA sensing facilitated reliable distributed measurements along the beam length. These findings indicate that the pi-bracket sensor system presents a promising and practical solution for SHM of bridge infrastructure, particularly in critical regions susceptible to fatigue cracking.

Future research directions may include comparative analysis of girder strain profiles under two loading conditions, first resulting in crack openings of 0.2 mm, versus the same load applied to an uncracked girder. The primary objective would be to isolate and quantify the strain variations attributable solely to crack formation. To achieve this, the strain profile of the uncracked girder to be subtracted from that of the cracked girder under identical loading conditions. This approach effectively eliminates the influence of the applied load, revealing the strain signature specific to the presence and severity of the crack.

ACKNOWLEDGMENTS

The authors would like to express their sincere gratitude to Research Manitoba for providing the necessary funding to support this project. Additionally, we appreciate the administrative support provided by Charleen Choboter, whose assistance has been invaluable throughout the project’s duration and beyond.

REFERENCES

[1] Mufti A., Thomson, D., Inaudi, D., Vogel, H. M. & McMahon, D. Crack detection of steel girders using Brillouin optical time domain analysis. Journal Civil Structural Health Monitoring. (2011) 1: 61-68. 2011.

[2] Lydon, M., Taylor. S.E., Robinson, D., Mufti, A. & O’Brien, E. J. Recent developments in bridge weight in motion (B-WIM). Journal of Civil Structural Health Monitoring 6, 69-91. 2016.

[3] Raeisi, F., Mufti, A., and Thomson, D. J. A finite-element model and experimental investigation of the influence of pre-straining of wire on the sensitivity of binary crack sensors. J. Civil Struct. Health Monit., 8(4), 673-687. 2018.

[4] Mufti, A. A. Structural health monitoring of innovative Canadian civil engineering structures. Struct. Health Monit., 1(1), 89-103. 2002.

[5] Raeisi, F., Mufti, A., Algohi, B. and Thomson, D. J. Placement of distributed crack sensor on I-shaped steel girders of medium-span bridges, using available field data. Structural Control Health Monitoring. 2019 (26). 2019.

[6] Roctest. DiTeSt SMARTape II Strain Sensor. n.d.

[7] Ettouney, M. M., and Alampalli, S. Infrastructure health in civil engineering: Theory and components. Springer, New York. 2012.

[8] Russo, F. M., Mertz, D. R., Frank, K. H., and Wilson, K. E. Design and evaluation of steel bridges for fatigue and fracture – Reference manual. Report No. FHWA-NHI-16-016, U.S. Department of Transportation, Federal Highway Administration, National Highway Institute, Washington, DC. 2016.

[9] Tokyo Sokki Kenkyujo Co., Ltd. Pi Gauge for Crack Width Measurement: PI-5-100, PI-5-200. 2024.

[10] Federal Highway Administration (FHWA). *Steel Bridge Design Handbook: Design for Fatigue and Fracture*. FHWA-IF-12-052 – Vol. 12, November 2012.